



Testing marine data assimilation in the northeastern Baltic using satellite SST products from the Copernicus Marine Environment Monitoring Service

Mihhail Zujev* and Jüri Elken

Department of Marine Systems, Tallinn University of Technology, Akadeemia tee 15A, 12618 Tallinn, Estonia

Received 14 August 2017, accepted 2 January 2018, available online 5 June 2018

© 2018 Authors. This is an Open Access article distributed under the terms and conditions of the Creative Commons Attribution-NonCommercial 4.0 International License (<http://creativecommons.org/licenses/by-nc/4.0/>).

Abstract. Satellite SST products from the Copernicus Marine Environment Service were tested for data assimilation in the sub-regional marine forecasts. The sub-regional setup of the HBM model was used in the northeastern Baltic, covering also the Gulf of Finland and the Gulf of Riga. Two assimilation methods – successive corrections and optimal interpolation – were implemented on the daily forecasts from April to December 2015. Independent daily FerryBox data from the ship track between Tallinn and Helsinki were used for validation. Higher SST forecast errors of the reference model were found near the shallower northwestern coasts. During the calm heating period in spring and early summer, the reference model produced in these regions too warm waters compared with the satellite and FerryBox observations. Too cold waters, compared to the observations, were modelled during the cooling period from late summer to winter. Although data assimilation reduced these errors, improving the treatment of coastal–offshore exchange in the core forecast model would be useful.

Key words: remote sensing, data assimilation, successive corrections, optimal interpolation, short-term forecast, HBM model, SST assimilation.

1. INTRODUCTION

Assimilation of observational results into oceanographic forecast models has a history of several decades, following with some delay developments of data assimilation in meteorology. In parallel to statistical forecast correction methods based on linear filtering and prediction theories (e.g. Kalman and Bucy, 1961), Cressman (1959) proposed a robust ‘manually tunable’ method directly applicable for correcting weather forecasts. Meteorology reached the state of working operational assimilation and forecast systems already in the 1970s (McPherson et al., 1979). In oceanography, only a few offshore regular time series observations have

been made. Shipborne observations, which provide most of the water column data, are non-synoptic and usually separated by a distance larger than the scale (size) of mesoscale motions. About a decade later than in meteorology, the first global oceanic data assimilation system (Derber and Rosati, 1989) was proposed based on sea surface temperature (SST) observations from merchant ships; quite sparse profile data from XBT, CTD, and Nansen bottles were incorporated as well.

Acquisition and assimilation of remote sensing data have been a common procedure for both meteorology and oceanography. However, the data coverage and accuracy are different for the atmosphere and the ocean. Reliable spaceborne thermal emissivity observations started in the 1960s on terrestrial (Buettner and Kern, 1965) and ocean (Anding and Kauth, 1970) surfaces.

* Corresponding author, mihhail.zujev@ttu.ee

Further, atmospheric infrared and microwave sounding allowed estimation of temperature and humidity profiles with height, also in the cloudy areas. Operational assimilation of remote sensing data into the weather forecast models was introduced in the 1970s, based on the adding of interpolated difference between observed and forecast values to the original forecast in order to obtain a corrected model state for the next forecast interval. The tests showed (e.g. Ghil et al., 1979) that the impact of data assimilation is highly sensitive to the quantity of data available; the choice of the assimilation method to determine the interpolation weights is also of importance.

Ocean sea surface temperature (SST) can be determined by most satellite sensors only in the cloud-free areas. Again, the amount of ocean data on the surface is irregular both in time and space as these are temperature–depth profile data; this causes significant problems in ocean data assimilation, compared with the more regular atmospheric observational data. Skin-layer corrected accurate (Donlon et al., 2002) and operationally available SST data that have high resolution both in space (<10 km) and time (6–12 h) have been synthesized and used for data assimilation since the beginning of the 2000s (Tang et al., 2004; Brasseur et al., 2005).

New remote sensing SST products were developed and made publicly available during the MyOcean project (Nardelli et al., 2013). This procedure is further developed and continued as the Copernicus Marine Environment Monitoring Service (CMEMS), <http://marine.copernicus.eu/>, providing Level 3 (or L3, supercollated or merged multisensor data, different options are available) and Level 4 (or L4, gap-free, interpolated from L3) SST products (Martin et al., 2012) in numerical format. These data open up new possibilities for operational data assimilation.

Statistical methods for data assimilation have many variants (e.g. Ide et al., 1997), which are all based on the estimated spatial–temporal correlation functions and variance fields. While optimal interpolation, 3DVAR, and 4DVAR methods assume in most applications prescribed statistical fields, then Kalman filters estimate and predict their variations depending on the evolution of oceanographic state variables. Good estimations are found when true ensemble forecasts can be made, with parallel forecasts starting from slightly modified initial conditions. Another option, demanding much less computing power, is to generate pseudo-ensembles from a single forecast. Sea level innovations, introduced by the assimilation procedure, propagate fast as barotropic long gravitational surface waves, therefore continuous assimilation with small increments during an assimilation cycle is advisable. Assimilation of temperature and/or salinity modifies the forecast density field, corres-

ponding perturbations propagate much slower as baroclinic internal waves or advective plumes; hence larger innovations are acceptable. When observations of different state variables are combined into the same forecast, multivariate optimal interpolation provides reliable results (Cummings, 2005).

In the Baltic Sea, probably the first data assimilation system was made by Sokolov et al. (1997) for ‘smart’ interpolation of temperature, salinity, and chemical profile data from monitoring stations, using a hydrodynamic model. Some tests have been devoted to assimilation of sea level data (Canizares et al., 2001; Sørensen and Madsen, 2004; Ivanov et al., 2012), based on the various options of the Kalman filter.

Assimilation of scalar variables such as temperature and salinity into the Baltic Sea models has a quite rich history. The present study has some specific features. Firstly, assimilation is designed into the operational forecast system and is prepared for the routine use; therefore, the methods must be robust and computationally effective. Secondly, the study is based on the downstream forecasts from the Baltic-wide core service system and both the model results and SST observations are of high spatial resolution. However, in the present study we deal with the validation of averaged data sets and do not consider high-resolution details.

Earlier, the operational assimilation system presented by Funkquist (2006) used 3D optimal interpolation (3D OI) for satellite and profile data. Correlation functions, needed for OI, were also estimated by Høyer and She (2007), She et al. (2007), and Fu et al. (2011a). Nowicki et al. (2015) used the Cressman method of successive corrections (SC) for satellite-based SST data. A number of pre-operational experiments have been conducted to test the performance of new assimilation methods: 3DVAR with isotropic (Zhuang et al., 2011) and anisotropic (Liu et al., 2009) recursive filters to estimate covariance functions, Ensemble Optimal Interpolation (Fu et al., 2011b), Singular Evolutive Interpolated Kalman Filter (Losa et al., 2012, 2014). Long-term reanalysis studies have used SC (Axell, 2013), 3DVAR (Fu et al., 2012; Fu, 2016), Ensemble Optimal Interpolation (Liu et al., 2013, 2014), and Ensemble 3DVAR (Axell and Liu, 2016).

This study is aimed at testing marine data assimilation into the operational high-resolution sub-regional forecast model of the northeastern Baltic, using new, routinely available satellite SST products from the CMEMS. The paper starts with the presentation of the model, data, and methods. The results section considers satellite data comparison with FerryBox, spatial, and seasonal features of assimilated data. Model skill estimates are given for the free run without assimilation, and for the model run with different options of

assimilation. We discuss possible ways to use less costly assimilation methods, yielding the results of nearly the same quality as with more sophisticated methods. Finally, conclusions are presented.

2. MODEL, DATA, AND METHODS

2.1. Sub-regional marine forecast model HBM

For assimilation tests we used the HBM-EST model (Lagemaa, 2012), which is an Estonian implementation of the HBM model (the abbreviation comes from HIROMB-BOOS Model). The model was originally constructed by the Bundesamt für Seeschifffahrt und Hydrographie, Hamburg, Germany, named as BSHCmod. Further developments have been made within Baltic-wide cooperation in operational forecasting; different options were merged to a new thoroughly tested HBM code within the EU MyOcean project. Details of the HBM model and its implementation are given by Berg and Poulsen (2012).

The HBM is a free-surface baroclinic 3D ocean model written in geographical latitude/longitude spherical coordinates that uses a horizontal staggered Arakawa C-grid and a fixed vertical grid with variable spacing and time-varying top layer thickness. There is also an option for dynamical vertical coordinates where the grid spacing changes in time. Vertical turbulence is treated by the κ - ω turbulence model and horizontal turbulence is treated within the well-known Smagorinsky formulation. The sea ice module is an integrated part of the HBM model, including both dynamics and thermodynamics. The model can take into account the results from independent wave models.

The forcing of the model is done by externally prescribed surface fields, point sources, and open boundary conditions. Surface fields are adopted from the numerical weather prediction model: 10-m wind components, mean sea level atmospheric pressure, surface air temperature, surface air humidity, and cloud cover. The HBM model calculates surface energy fluxes (mechanical, radiative, thermodynamic) using bulk parameterization formulae. Point source data are freshwater fluxes from rivers. If actual discharge forecasts are missing, the climatology for each calendar day will be used.

On the ocean side, the HBM model is forced by the tidal sea surface elevation, sea level forecasts from the barotropic storm surge model of the Northern Atlantic, and monthly climatological hydrography. The Baltic Sea implementation of the HBM uses a nested approach: the largest area of the 3D forecast covers the North and Baltic seas with a grid step of 12 nautical miles, the intermediate resolution with a grid step of 3 nautical

miles is further refined into a 1-mile grid covering the whole Baltic Sea. In the Danish Straits, two-way nesting with a finer grid model with the resolution of 0.5 nautical miles is used.

The Estonian implementation of the HBM (Lagemaa, 2012) covers the Baltic Sea sub-area east from 21.55°E (Fig. 1), including the Gulf of Finland and the Gulf of Riga, with the resolution of 0.5 nautical miles. The horizontal grid of the HBM-EST model consists of 425 by 529 grid points. The grid cell length by longitude is 1', by latitude it is 30". In the vertical grid, 39 depth layers are used, with a 3-m grid step near the surface and larger grid steps in the deeper layers. Forcing at the western open boundary is taken from the Baltic-wide HBM model, which operates routinely within the CMEMS with the resolution of 1 nautical mile. Forcing on the sea surface is obtained from the Estonian version of the HIRLAM model that is run by the national weather service for operational forecasts on a 11-km grid. For analysis of observation and forecast errors in relation to wind conditions, time series of wind speed components were extracted in the central part of the Gulf of Finland.

We chose the year 2015 for the forecasting and assimilation experiment. The forecasts were updated daily by introducing a new weather forecast at midnight.

2.2. Satellite SST data

Sea surface temperature data, observed from satellites, were used as input observational data within data assimilation. Gridded observation maps were obtained from the CMEMS multi-sensor product, which is built from bias-corrected L3 mono-sensor products at the horizontal resolution of 0.02 by 0.02 degrees. For each day a single SST value was used, which was reduced to midnight based on available observations at different times (near-real-time).

This product (Bonekamp et al., 2016) contains results from the merging of various satellite SST level 2 data, which have passed a significant number of quality controls and which have been calibrated through an inter-sensor bias correction procedure to provide an estimate of the night time SST based on original SST observations without any smoothing or interpolation. Details of the product are described on CMEMS web resource <http://cmems-resources.cls.fr/documents/QUID/CMEMS-OSI-QUID-010-009-a.pdf>.

Sensors used include METOP_B, SEVIRI, VIIRS_NPP, MODIS, and others. Observations were collected from different producers: NASA, NOAA, IFREMER, EUMETSAT OSI-SAF, and ESA.

Depending on the cloud cover there were from 200 up to 21 000 observations per day. Some obviously erroneous SST values (which differed more than 10 K

from model ones) were filtered out. All of them were used for the assimilation with the Cressman method. For optimal interpolation a data thinning algorithm was implemented, leaving one value for the area of 2.5 by 5 nautical miles.

An example of data extracts is shown in Fig. 2a, representing the observations on the line between Tallinn and Helsinki during the whole test period. The temperatures presented here are averaged over one week.

2.3. FerryBox data

Automatic observations made from ships crossing the sea areas were used as independent data for validation and quality assessment. FerryBox is a measurement system installed on board commercial ferries that collects temperature, salinity, chlorophyll *a* fluorescence, and turbidity data. This technology is used to study basin-scale temperature and salinity patterns together with mesoscale processes and upwellings (Kikas and Lips, 2016). The water is sampled at about 4 m below the surface at different rates and every 20 s the measurement is recorded, thus covering roughly 160–200 m in the horizontal direction. There are quality check procedures to eliminate unexpected and physically unrealistic values; cross-checking with the same data from the return trip is performed as well (Kikas and Lips, 2016). Detailed description of technical features of the FerryBox system is given by Lips et al. (2008).

Observations are available on the route Tallinn–Helsinki on the forth and back tracks twice a day with a time step of 20 s. Temperatures on the same latitude were averaged across multiple tracks. For each day one mean SST value was calculated regardless of the time of the day and the number of observations in the particular grid cell. Weekly averages of the temperatures observed by the FerryBox system are shown in Fig. 2b.

The data were taken as they are within the Copernicus system, in which the procedures include an advanced quality check. As our aim was to check the working of automatic systems, no additional quality control or processing was performed.

2.4. Data assimilation

Let us consider the model state represented by a vector $\mathbf{x} = \{u, v, T, S, \rho, \xi, \dots\}$, where the values in brackets are the model state variables (velocity components, temperature, salinity, water density, sea level, etc.), generally given at discrete grid points. When the model predicts the state vector \mathbf{x}_b on m grid points, it has some errors regarding the true state. Observations \mathbf{y}

are taken usually at different n locations than \mathbf{x}_b . Assimilation is a procedure to create the analysis vector \mathbf{x}_a on the same set of coordinates as \mathbf{x}_b with a condition that by a given set of criteria, \mathbf{x}_a is closer to \mathbf{y} than \mathbf{x}_b . When the model state values $\hat{\mathbf{y}}$ in the points of observations are obtained by an interpolation procedure, then the analysis is calculated from the innovation vector $\mathbf{y} - \hat{\mathbf{y}}$ by the formula

$$\mathbf{x}_a = \mathbf{x}_b + \mathbf{K}(\mathbf{y} - \hat{\mathbf{y}}), \quad (1)$$

where \mathbf{K} is the gain matrix containing $m \times n$ weights for interpolation over $1 \times n$ observation points. At individual model grid point i formula (1) can be written using the weight vector $\mathbf{w}_i = (\mathbf{K})_i$. In the following formulae we consider one state variable only and omit the index i , describing the specific model grid point. As a result we obtain

$$x_a = x_b + \mathbf{w}(\mathbf{y} - \hat{\mathbf{y}}) = x_b + \sum_{j=1}^n w_j (y_j - \hat{y}_j). \quad (2)$$

2.4.1. Successive corrections

The successive correction method or the Cressman (1959) method assumes univariate relations between the state variables and that weights of the individual observations w_j in (2) decrease with the distance d_j between the observation point j and the model grid point i . Let us define the influence radius R around the model point i , where k observations out of total n observations are located. Good assimilation results are obtained with the weights given by the formula

$$w_j = \frac{\max\left(0, \frac{R^2 - d_j^2}{R^2 + d_j^2}\right)}{\left[\sum_{j=1}^n \max\left(0, \frac{R^2 - d_j^2}{R^2 + d_j^2}\right) + \eta^2\right]}, \quad (3)$$

where the weights are positive within the influence radius and zero elsewhere. Reduction of the assimilation weights in real noisy conditions is done by introducing relative noise variance η^2 , estimated from the variances of observation errors σ_o^2 and background errors σ_b^2 , $\eta^2 = \sigma_o^2 / \sigma_b^2$. In the noiseless case ($\eta^2 = 0$) the sum of weights is equal to unity.

Data assimilation for SST was made using a medium-scale value 37 km (20 nautical miles, 40 grid points) for the influence radius. This length is about ten times larger than the Rossby deformation radius. Therefore, the impact of individual mesoscale eddies is suppressed, but basin-scale SST features are kept. The weight function has the greatest impact within the nearest 5 km, then it goes almost linearly to zero for 37 km. Before

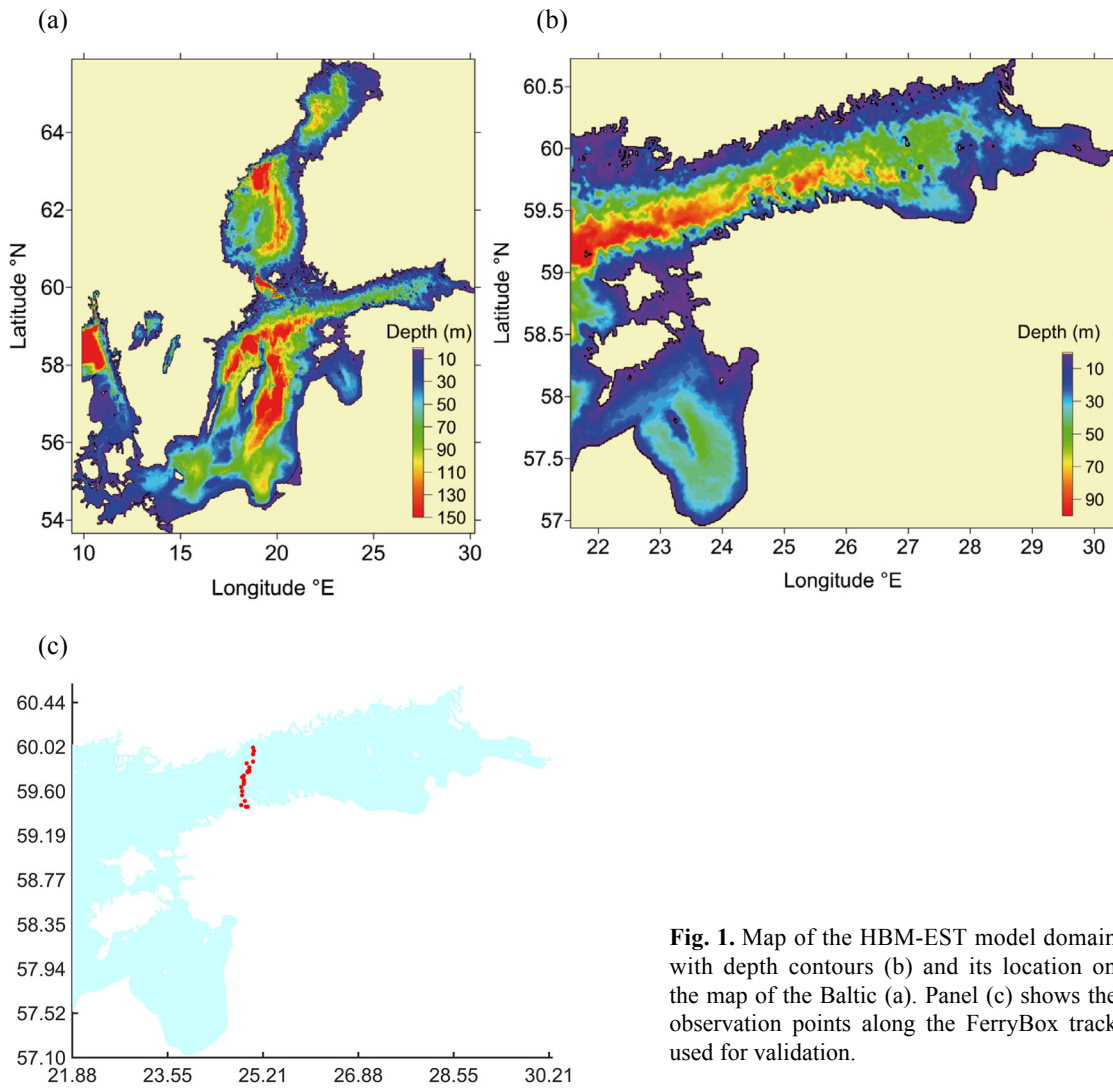


Fig. 1. Map of the HBM-EST model domain with depth contours (b) and its location on the map of the Baltic (a). Panel (c) shows the observation points along the FerryBox track used for validation.

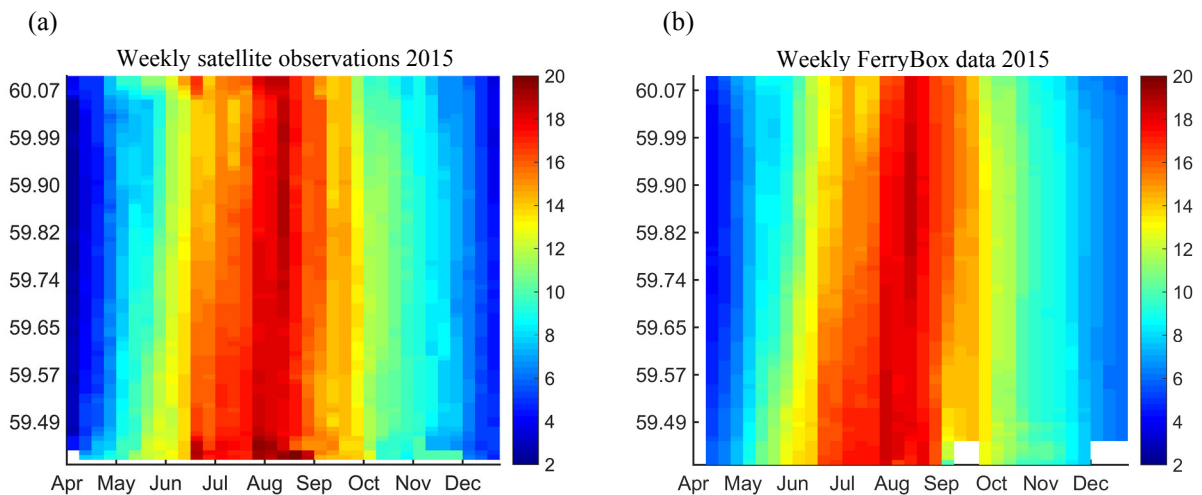


Fig. 2. Time–latitude map of the weekly mean sea surface temperature observed from satellites (a) and FerryBox (b) between Tallinn (south) and Helsinki (north).

assimilation, the observations were averaged over each grid cell in order to avoid oversampling problems. During the testing of the scheme, the values of σ_o^2 and σ_b^2 were not known in advance. For the chosen data set we obtained acceptable results with $R = 37$ km and $\eta^2 = \sigma_o^2/\sigma_b^2 = 2$. We used these values throughout the entire model run.

For computational efficiency, assimilation was performed in the two-dimensional domain for the surface layer only; deeper model levels were left unaffected. Since the observations were assimilated every day, the introduced innovations were moderate (compared to the vertical mixing) and not visible in the graphs of vertical profiles.

2.4.2. Optimal interpolation

Optimal interpolation as developed by Gandin (1963) uses least-square minimization of analysis errors to calculate the weight coefficients w_j in expression (2). We follow the original point-wise presentation (see also Høyer and She, 2007) and denote $f_j = y_j - \hat{y}_j$, $f_0 = \tilde{x}_a - x_b$. Here \tilde{x}_a is the ‘true’ unknown state in the model point i . The observations include random errors ε_j ; the error variance is $\sigma_{\varepsilon_j}^2$. The squared interpolation error, averaged over an ensemble,

$$E = \left[f_0 - \sum_{j=1}^n w_j (f_j + \varepsilon_j) \right]^2 \Rightarrow \min \text{ is minimized with}$$

respect to w_j . This is achieved by setting n constraints for the derivatives $\partial E / \partial w_j = 0$, using the conditions $f_j = 0$, $f_0 = 0$, $\varepsilon_j = 0$, $\varepsilon_j f_j = 0$, $\varepsilon_j f_0 = 0$. As a result, we obtain for the i th model point the following system of n linear equations regarding w_j :

$$\sum_{j=1}^n \overline{f_k f_j} w_j + \sigma_{\varepsilon_k}^2 w_j = \overline{f_k f_0}, \quad k = 1 \dots n, \quad (4)$$

which can be easily solved. By dividing equations (4) by the variance $\sigma_f^2 = f_k^2$, we obtain correlation instead of spatial covariance. The weight coefficients of optimal interpolation are determined by the correlation matrix between the individual observation points $\mathbf{B} = \{\overline{f_k f_j} / \sigma_f^2\}$ and the correlation vector between the observation point and the i th model point $\mathbf{b} = \overline{f_k f_0} / \sigma_f^2$, and by the relative variance of observation error $\eta^2 = \sigma_{\varepsilon_k}^2 / \sigma_f^2$. Equation (4) can be rewritten as $\mathbf{w}(\mathbf{B} + \eta^2 \mathbf{I}) = \mathbf{b}$, where \mathbf{I} is a unit matrix. The vector of weights is calculated in the form

$$\mathbf{w} = \mathbf{b}(\mathbf{B} + \eta^2 \mathbf{I})^{-1}. \quad (5)$$

More general matrix-vector formulations of optimal interpolation can handle also the case where observation errors may be correlated between each other and with

the background field (Lorenç, 1986; Ide et al., 1997). However, most of the practical implementations, like in our case, are limited to equations (4) with solution (5), where the spatial correlation is prescribed as a function with ‘tuned’ parameters.

Correlations \mathbf{B} and \mathbf{b} were approximated by the Gaussian function from the distance r between the correlated points. Anisotropic correlation features were taken into account by the directional distribution of the correlation scale from the angle θ in the form of the ellipse dependence $L = a \sin(\theta - \theta_0) + b \cos(\theta - \theta_0)$ relative to the reference angle θ_0 . So the correlation was adopted in the form $B(r, \theta) = \exp(-r^2 / L^2(\theta))$, where $L = L(\theta)$ was pre-calculated in each model grid point according to the coastline and topography. Following the results by Høyer and She (2007), longer correlation scales were adopted along the coasts and the isobaths than in the perpendicular direction. The typical horizontal impact scale along the coast or isobath was chosen as 15 km. Standard deviations for the entire run were taken $\sigma_o^2 = 0.5$ and $\sigma_m^2 = 1.0$.

Before performing the assimilation according to equations (2) and (5), the observations were filtered with a thinning algorithm to avoid oversampling and a huge computation amount, leaving up to $n = 700$ points. The distance between the generated super-observations was kept at 10 km or more. For computational efficiency, wet points (located in the sea) were divided into 30 blocks to cover the entire basin. That leaves up to 81 observations per block. Observations from each block were cross-compared with all other observations in the same block plus the neighbouring observations falling into the adjacent area within a radius of 100 km, and the correlation coefficients were calculated.

2.5. Methods for data quality and model skill assessments

There are a number of different SST data sets that can be compared. Here remote sensing SST products (SAT) from CMEMS are used for data assimilation. FerryBox observations (FB), carried out by the Department of Marine Systems but accessed from the Copernicus service, provide independent data for the assessment of the skill of data assimilation. Before estimating the skill of model versions (without data assimilation or with different assimilation options) in reference to one or another observational data set, the observations from different platforms are compared.

Following the approach by Taylor (2001), for each comparison of the two variables f_n and g_n a common data set is defined where missing values of one or both data sets are ignored. If the standard deviations of the

data sets are σ_f , σ_g and the coefficient of their mutual correlation is $R_{f,g}$, then the centred (with bias removed) root-mean-squared difference (RMSD) of the data sets E' will read

$$E'^2 = \sigma_f^2 + \sigma_g^2 - 2\sigma_f\sigma_g R_{f,g}. \quad (6)$$

The size of the original data sets is very different. Therefore we reduced in many cases the compared data sets to the FerryBox transect between Tallinn and Helsinki. Such data form a time–latitude matrix with a daily step in time and a 2.222 km step by latitude. For the data gap treatment we used the weekly average of all the available data. The missing values were just omitted from the averaging. Since satellite data were recalculated to the midnight values, for this comparison the forecast was treated as the weekly average of nightly (23 h advance) values. Other data set definitions are explained in the results section when necessary.

The model data sets are named as FR ('free' model run without data assimilation), SC (model run with assimilation of Copernicus SST with successive correction method), and OI (model run with assimilation of Copernicus SST with the optimal interpolation method). The model data sets have 71986 values for each time step.

3. RESULTS

3.1. Comparison of SST from satellite and FerryBox

There are principal differences between the temperature observed from satellites and from in situ sensors located a few metres below the surface. These observations give closer results in well-mixed conditions (Siegel et al., 2006; Uiboupin and Laanemets, 2015), which occur during stronger winds.

Here we compare averaged satellite observations from the Copernicus service (SAT) during 2015 along the FerryBox track with the in situ data of the latter (FB). Temperature values were merged by latitude, leaving out the impact of ship track variations. Several values for the same bin were replaced by their mean. The SAT data were provided as of midnight while the FB observations were made at different times during a particular day. The FB data represent the average temperature in the upper mixed layer, whose depth is variable. The data sets are independent of each other and have their maxima in August.

The difference between the two SST data sets is shown in Fig. 3. In central parts of the Gulf of Finland (latitudes 59.5–60 N) there is a clear seasonal behaviour. The thin layer temperature registered by the satellite was 0.3–0.7 K larger than the bulk temperature of the

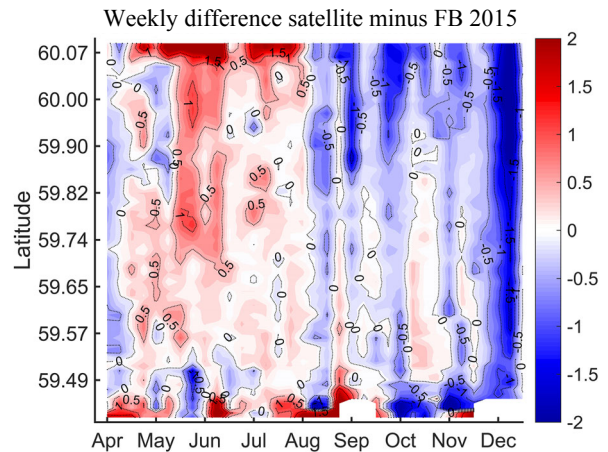


Fig. 3. Weekly mean sea surface temperature difference between the satellite and FerryBox observations on a transect between Tallinn (south) and Helsinki (north) as a function of time and latitude.

upper layer (observed at 4 m depth) during spring and summer until August but insignificantly (less than 0.5 K) smaller in autumn and early winter. Larger SAT minus FB differences emerged occasionally in areas close to the coasts: a range 0.7–1.0 K was observed in Tallinn Bay and a larger range, 1.0–2.5 K, was found near Helsinki. In December the thin surface layer cooled down by 0.5–1.5 K more than the deeper surface layer along the whole transect, including also the coastal waters.

In most of the cases the difference between the two data sets (SAT minus FB) was of the same sign over the whole transect. This is consistent with the results by Uiboupin and Laanemets (2015), who studied similar data from 2000–2009. They found that during wind speeds less than 5 m/s different satellite sensors give up to 3 K larger SST than it is observed by FB; the difference is largest at smaller wind speeds of 2 m/s and less during temporary stratification of the thin surface layer. In our case with CMEMS data the difference was larger near the coasts, but both the coastal areas usually appeared in the SAT data either warmer or colder than it was found from the FB data. The reasons for large SST differences between satellite and in situ observations were discussed by Siegel et al. (2006). They also noted a seasonal behaviour as it is evident from our data presented in Fig. 3.

3.2. Spatial patterns of SST

Sea surface temperature patterns manifest a variety of physical processes like different heating or cooling in coastal versus offshore areas, coastal upwelling, thermal fronts between the water masses, and signatures of mesoscale eddies and filaments.

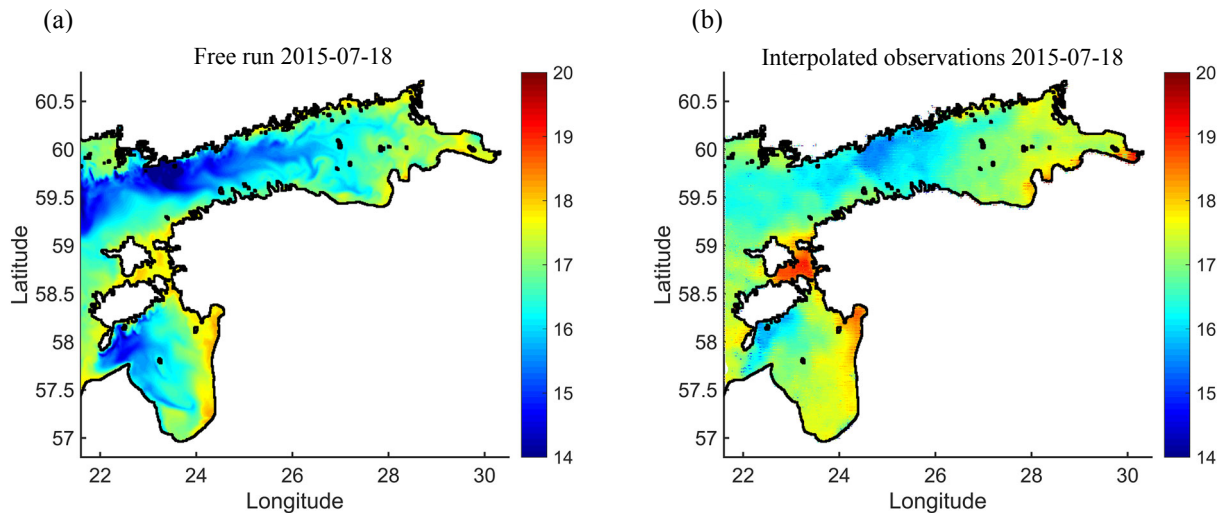


Fig. 4. Example of a HBM forecast (a) and satellite observations interpolated on the same grid (b). Both data from 2015-07-18.

We present an example of SST distributions for a summer date when there was good coverage of the sea area with satellite data. Comparison of the results of the model forecast (Fig. 4a) and remote sensing (Fig. 4b) reveals a different extent of warmer and colder areas of coastal waters. Model results show wide bands of colder water off the northern coasts, both in the Gulf of Finland and the Gulf of Riga. Satellite data registered only a small fraction of these colder water masses. In the warmer shallow areas, located between the Estonian larger islands and near the eastern coast of the Gulf of Riga, satellite observations yielded higher SST (by about 1 K) than the model. This can be partly attributed also to the wind-dependent positive bias of satellite data (Uiboupin and Laanemets, 2015). We note that the model reproduces in the above example more distinct mesoscale patterns than are evident from the satellite data.

3.3. Time series of SST

In the adopted data assimilation approach, SST satellite observations (example given in Fig. 4b) are used to correct the model forecast (example given in Fig. 4a). FerryBox data are independent and intended for validation. The data as defined in Section 2 are from observations (SAT and FB) and from models (FR, SC, and OI). The data are compared on the FerryBox transect (see Fig. 1c), where all the data are available. The model results are with a regular time interval (1 h), but daily observations have gaps.

In the open part of the Gulf of Finland daily SAT data from CMEMS (Fig. 5a) revealed generally higher

temperatures than FB during the warming period (see also Fig. 3). The SAT data were spiky compared with the FB data: warmer spikes occurred during the warming period and colder spikes during the cooling. The FR forecast provided in the offshore waters slightly smaller SST than observed. Data assimilation using SC and OI ‘dragged’ the model results towards SAT observations, still the SST spikes did not appear in the assimilated model results.

As the cross-gulf SST pattern (Fig. 5b) shows, the southern part of the gulf warmed up faster than the central and northern parts, based on the results from SC-assimilated model data (see also weekly SAT and FB data in Fig. 2). This resulted in warmer by up to 5 K waters on a specific day. Cooling took place more uniformly across the research area, temperature differences were up to 1.5 K. Similar regional differences were evident in other data sets.

3.4. Skill assessment for non-assimilated and assimilated model results

Independent FB data obtained in a cross-section of the Gulf of Finland form the most comprehensive off-shore in situ data set within the forecast area. In the following we compare the assimilated model results obtained using the two methods with the FB data. For the non-assimilated model data (FR, reference run) we present comparisons for model validation. Since the two observations, SAT and FB, have different SST values (see Section 3.1), comparison is also made in reference to remote sensing data that were used in the assimilation process.

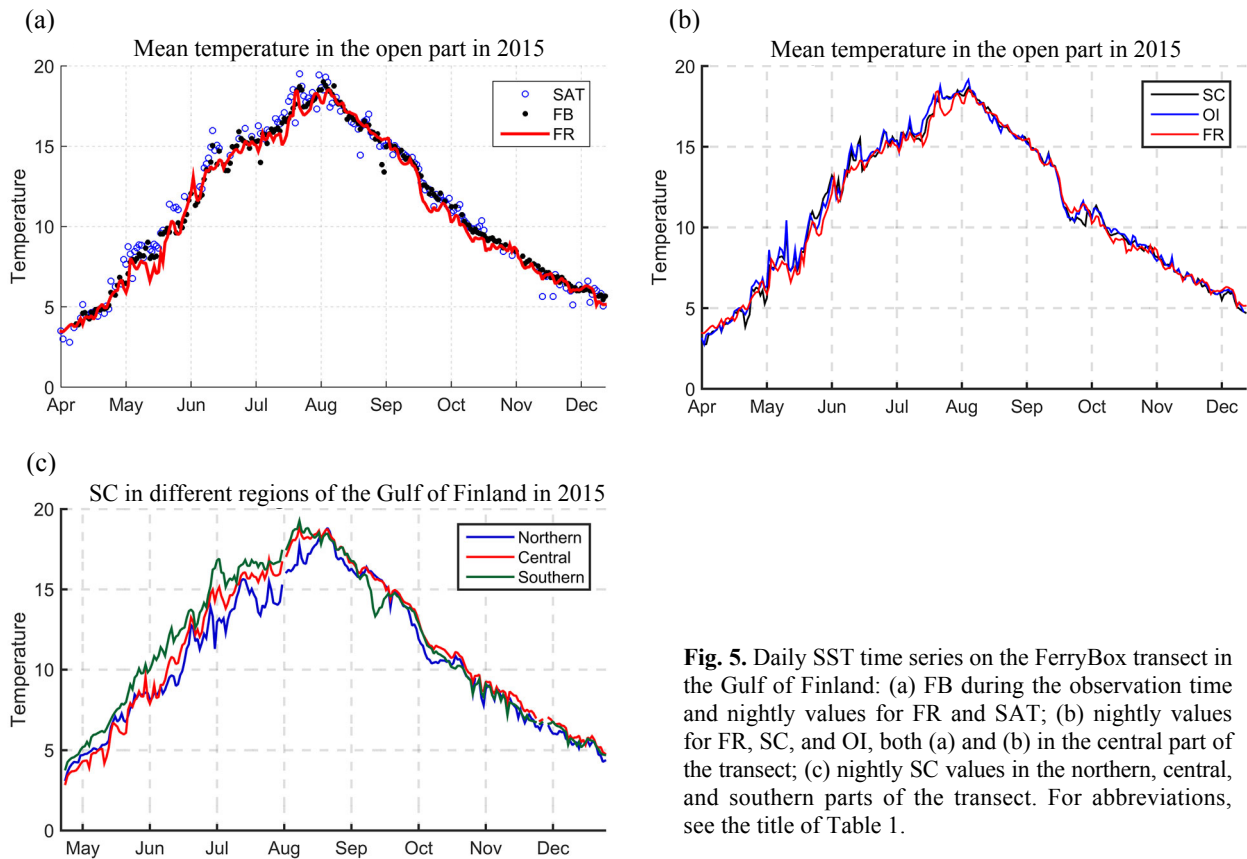


Fig. 5. Daily SST time series on the FerryBox transect in the Gulf of Finland: (a) FB during the observation time and nightly values for FR and SAT; (b) nightly values for FR, SC, and OI, both (a) and (b) in the central part of the transect; (c) nightly SC values in the northern, central, and southern parts of the transect. For abbreviations, see the title of Table 1.

Further we consider temporal evolution of cross-gulf SST patterns in the Gulf of Finland on the basis of weekly average transects. Since the SAT data are from midnight, we used nightly model data for finding the weekly averages. The difference between the daily mean and nightly model values (not shown) due to the diurnal cycle was up to 0.5 K from April to August and slightly negative from September to December.

Both the SC and OI methods gave similar patterns of differences relative to FB data (Fig. 6). These patterns are similar to that of FR minus FB (not shown), but the variations of difference have been reduced by the data assimilation. Greater differences were found in the northern part of the Gulf of Finland, where a positive difference was evident from April to August (although the SC method gave some shorter negative differences as well) and a negative difference from September to December. In the central part of the gulf data assimilation corrected the errors of FR effectively and the forecast absolute difference from the FB data was in most cases less than 0.5 K. Exceptions were found during stronger winds at the beginning of October and November, when the assimilated SST forecast remained by about 1 K smaller than FB observations. Positive anomalies were

observed during the periods of calmer winds in the second half of May and August. Comparison of the results by SC and OI methods indicates that OI provided with a given set of parameters generally smaller differences from FB than SC, except in June and July near the northern coast when OI produced larger differences than SC. We note that the SC method used the interpolation weights not dependent on the direction between the points; in case of OI longer correlation scales were used along the coasts than in the cross-shore direction.

Within the data assimilation, greater changes in reference to FR (Fig. 7) were made by the OI than by the SC method. We selected the OI parameters on the basis of some trials. However, investigation of the best combination of different parameters for OI is outside the scope of this paper, reduction of sigma ratio $\varepsilon^2 = \sigma_o^2 / \sigma_m^2$ by the factor of two did not yield plausible results.

Statistical comparison of weekly mean values of the FR forecast and the assimilated SC and OI forecasts with FB data (Table 1) revealed that assimilation provided better correspondence to the independent observations. Based on formula (6), improvements are visible in bias, RMSD, and correlation R . The main skill estimator –

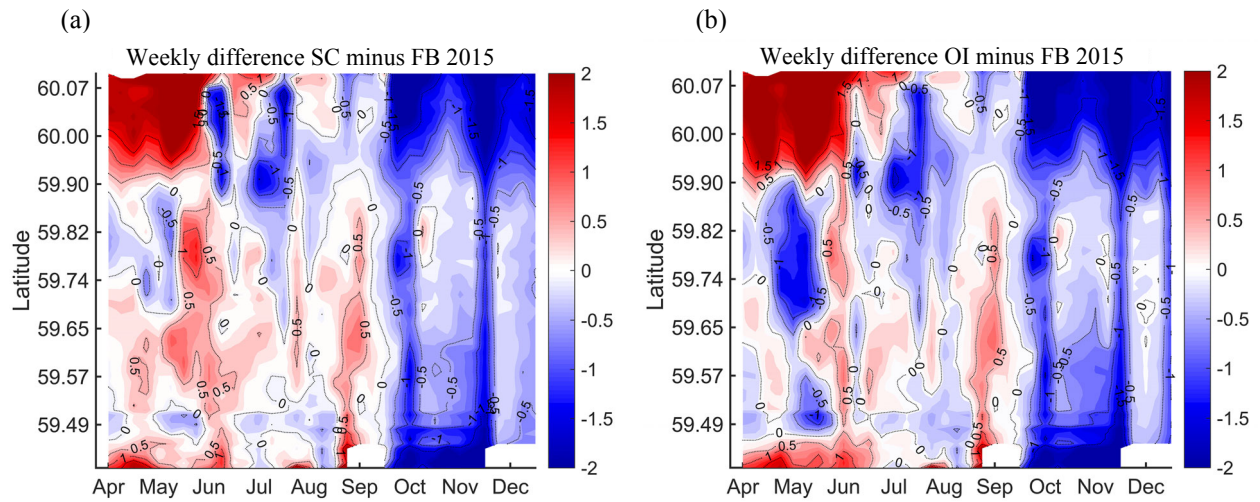


Fig. 6. Time–latitude map of the weekly mean sea nightly surface temperature difference of assimilated with SC (a) and OI (b) in reference to FerryBox data between Tallinn and Helsinki. For abbreviations, see the title of Table 1.

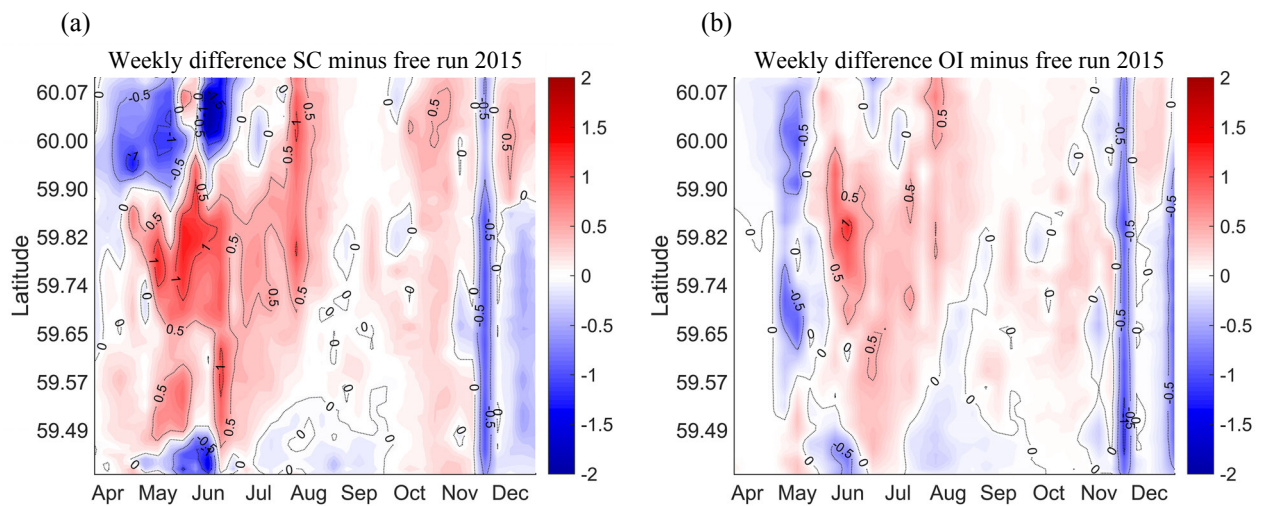


Fig. 7. Time–latitude map of the weekly mean nightly sea surface temperature difference of assimilated with SC (a) and OI (b) in reference to non-assimilated model data between Tallinn and Helsinki. For abbreviations, see the title of Table 1.

Table 1. Statistics of free model run without data assimilation (FR), model run with assimilation with the successive correction method (SC), model run with assimilation of Copernicus SST with the optimal interpolation method (OI), and remote sensing SST data (SAT) with reference to FerryBox data (FB)

	FR	SC	OI	SAT	FB
Bias	−0.45	−0.34	−0.42	−0.31	0
RMSD	0.97	0.84	0.96	0.66	0
Correlation R	0.931	0.937	0.934	0.936	1.00
Mean	10.99	11.11	11.03	11.13	11.45
Standard deviation σ	4.35	4.45	4.48	4.57	4.19

RMSD – was less than 1 K in all the cases, which can be considered acceptable. In the given selection of assimilation parameters, SC provided slightly better results than OI, that is SC had a smaller bias and RMSD and a larger correlation. Since the statistics was calculated in relation to the constant mean value over the whole data set (period from April to December), deviations contained the seasonal cycle. Therefore standard deviations of SST were in the range of 4.2–4.6 °C. This is also the reason why the calculated correlations were quite high – more than 0.93.

In reference to the SAT data, FR had RMSE =0.96. Data assimilation reduced this value to 0.82 (SC) and 0.93 (OI).

4. DISCUSSION

Massive validation of Baltic marine forecast products was conducted earlier by the Baltic Monitoring and Forecasting Centre. Results from different Baltic-wide model setups were compared with offshore and coastal in situ observations and with satellite L3 supercollated products. From the project report (<http://marine.copernicus.eu/documents/QUID/CMEMS-BAL-QUID-003-006.pdf>) it can be found that in the year 2008 a common feature of the present HBM model versions was faster heating during spring and summer and faster cooling during autumn. For example, comparison of the monthly mean SST maps from remote sensing (SAT) to the forecast SST maps reveals a positive bias of the model forecast of up to 2 K from April to July and a negative bias amounting to –1 K from September to December. During another period, in 2013, the bias was negative throughout the whole year, with largest forecast–observation differences found in winter. Spatial differences in the bias were evident as well. In the Gulf of Finland the forecast SST tends to be smaller than that observed by SAT data. In our study with the sub-regional model of higher resolution, a seasonally and spatially varying bias appears also in our FR data (reference run without data assimilation).

Compared to the errors in the open sea, higher modelled SST monthly and quarterly scale errors were found in our study in the coastal areas. A possible reason is that the model produces too fast heating or cooling in shallow coastal areas, where stratification is usually absent. This indicates probable underestimation of modelled coastal–offshore exchange. Recent studies emphasize the importance of sub-mesoscale exchange processes (Lips et al., 2016; Väli et al., 2017), which need to be adequately captured by the models. During the spring heating period, the SAT data taken from the surface showed higher SST in the coastal areas than the

FB data observed at 4-m depth (Fig. 3). This points to the importance of accounting for the shallow stratification that may develop during the calm days.

Another important forecast aspect in coastal areas is reproduction of upwelling events (Uiboupin and Laanemets, 2009; Laanemets et al., 2011). Although upwelling patterns are modelled quite well, models tend to produce too low temperatures near the northern coast of the Gulf of Finland compared to the SAT data. On the larger estuarine systems this mismatch may be related to the interaction of surface circulation (Elken et al., 2011; Soosaar et al., 2014) and lateral salinity gradients that create thin layers of less saline water on the surface during calm weather and suppress mixing; such layers may not be resolved well by the models.

Introduction of SAT data assimilation by the SC and OI methods slightly improved the forecast. However, since SAT and FB data sets of SST have differences, the assimilated model results kept to some degree the main error features relative to FB such as too warm waters in the northern part of the Gulf of Finland during the heating period in May and June and too cold waters on the whole Gulf of Finland cross-section during the cooling period from October to December. Usually OI provides more accurate results than SC, but in our case OI did not improve the forecast as much as SC. This may be due to the inadequate description of the correlation function and noise parameters. The focus of a further study could be improvement of the description of these parameters.

We tested routine tools – data products and standard, validated model – in the data assimilation into sub-regional ocean forecast models. The results were satisfactory, and there is a need and possibility for further developments that can be divided into two categories: improvements in data and in models. SAT products of SST are often too smooth and lack mesoscale details under cloudy areas. In such areas there is deviation of heat exchange with the atmosphere compared to cloud-free conditions and sometimes also heavy precipitation, which both cause anomalies in SST. If we assimilate SST towards SAT data, it may happen that the assimilation result will be more different from the independent FB data than the model results without assimilation. There could be a need for an algorithm to incorporate FB observations into the satellite-based SST product. The spatial effect of such correction is presently not known. The SST in coastal stations depends very much on very-high-resolution local topography, and these data can be used mainly in the local forecast models.

Both the used data assimilation algorithms have several important parameters that influence the forecasting of the key variables and yield results of different quality.

For this study these values were picked as the best choice to our knowledge compared to other options. However, this does not mean the results cannot be improved.

There is a challenge to use more observations for data assimilation, but there should be some reliable independent data remaining for validation. If FerryBox data could be used in combination with CMEMS SAT products, we would be left with sparse point observations from coastal stations for checking the quality of assimilation.

5. CONCLUSIONS

It was found that satellite SST products from the Copernicus Marine Environment Monitoring Service can be well used for data assimilation in the sub-regional marine forecasts. Although the reference model without data assimilation – sub-regional setup of the HBM model – provided SST forecasts with root-mean-square difference to the observational data sets (satellite products and independent FerryBox data) less than 1 K, further improvements of the forecast were achieved by robust implementation of two assimilation methods: successive corrections and optimal interpolation. Within the selected parameters of assimilation algorithms, a computationally effective successive corrections algorithm gave slightly better results in reference to independent FerryBox data than optimal interpolation.

Higher SST forecast errors of the reference model were found near the shallower northwestern coasts. During the calm heating period in spring and early summer, the reference model produced in these regions too warm waters compared with the satellite and FerryBox observations. Too cold waters, compared to the observations, were modelled during the cooling period from late summer to winter. Although data assimilation reduced these errors, improving the treatment of coastal–offshore exchange in the core forecast model should be useful.

ACKNOWLEDGEMENTS

Development of the HBM model was done by a larger BAL MFC team within the EU projects MyOcean, MyOcean2, and MyOcean-FO. Details of the model implementation were introduced by Priidik Lagema. Lars Axell from Swedish Meteorological and Hydrological Institute gave guidance on the data assimilation algorithms and kindly provided the FORTRAN codes. The study was supported by the PhD programme for Mihhail Zujev and institutional research funding IUT 19-6 of

the Estonian Ministry of Education and Research. The publication costs of this article were partially covered by the Estonian Academy of Sciences.

REFERENCES

- Anding, D. and Kauth, R. 1970. Estimation of sea surface temperature from space. *Remote Sens. Environ.*, **1**(4), 217–220.
- Axell, L. 2013. *BSRA-15: A Baltic Sea Reanalysis 1990–2004*. SMHI.
- Axell, L. and Liu, Y. 2016. Application of 3-D ensemble variational data assimilation to a Baltic Sea reanalysis 1989–2013. *Tellus A*, **68**, 24220.
- Berg, P. and Poulsen, J. W. 2012. *Implementation Details for HBM*. DMI Technical Report No. 12-11. Copenhagen.
- Bonekamp, H., Montagner, F., Santacesaria, V., Nogueira Loddo, C., Wannop, S., Tomazic, I., et al. 2016. Core operational Sentinel-3 marine data product services as part of the Copernicus Space Component. *Ocean Sci.*, **12**(3), 787–795.
- Brasseur, P., Bahurel, P., Bertino, L., Birol, F., Brankart, J. M., Ferry, N., et al. 2005. Data assimilation for marine monitoring and prediction: the MERCATOR operational assimilation systems and the MERSEA developments. *Q. J. Roy. Meteor. Soc.*, **131**(613), 3561–3582.
- Buettner, K. J. and Kern, C. D. 1965. The determination of infrared emissivities of terrestrial surfaces. *J. Geophys. Res.*, **70**(6), 1329–1337.
- Canizares, R., Madsen, H., Jensen, H. R., and Vested, H. J. 2001. Developments in operational shelf sea modelling in Danish waters. *Estuar. Coast. Shelf S.*, **53**(4), 595–605.
- Cressman, G. P. 1959. An operational objective analysis system. *Mon. Weather Rev.*, **87**(10), 367–374.
- Cummings, J. A. 2005. Operational multivariate ocean data assimilation. *Q. J. Roy. Meteor. Soc.*, **131**(613), 3583–3604.
- Derber, J. and Rosati, A. 1989. A global oceanic data assimilation system. *J. Phys. Oceanogr.*, **19**(9), 1333–1347.
- Donlon, C. J., Minnett, P. J., Gentemann, C., Nightingale, T. J., Barton, I. J., Ward, B., and Murray, M. J. 2002. Toward improved validation of satellite sea surface skin temperature measurements for climate research. *J. Climate*, **15**(4), 353–369.
- Elken, J., Nömm, M., and Lagema, P. 2011. Circulation patterns in the Gulf of Finland derived from the EOF analysis of model results. *Boreal Environ. Res.*, **16**, 84–102.
- Fu, W. 2016. On the role of temperature and salinity data assimilation to constrain a coupled physical–biogeochemical model in the Baltic Sea. *J. Phys. Oceanogr.*, **46**(3), 713–729.
- Fu, W., Høyer, J. L., and She, J. 2011a. Assessment of the three dimensional temperature and salinity observational networks in the Baltic Sea and North Sea. *Ocean Sci.*, **7**(1), 75.
- Fu, W., She, J., and Zhuang, S. 2011b. Application of an Ensemble Optimal Interpolation in a North/Baltic Sea

- model: assimilating temperature and salinity profiles. *Ocean Model.*, **40**(3), 227–245.
- Fu, W., She, J., and Dobrynin, M. 2012. A 20-year reanalysis experiment in the Baltic Sea using three-dimensional variational (3DVAR) method. *Ocean Sci.*, **8**(5), 827–844.
- Funkquist, L. 2006. An operational data assimilation system for the Baltic Sea. In *European Operational Oceanography: Present and Future* (Dahlin, H., Flemming, N. C., Marchand, P., and Petersson, S. E., eds). EuroGOOS Office, Norrköping, Sweden, and European Commission, Brussels, Belgium, pp. 656–660.
- Gandin, L. S. 1963. *Objective Analysis of Meteorological Fields*. Gidrometizdat, Leningrad. (English translation No. 1373 by Israel Program for Scientific Translations (1965), Jerusalem.)
- Ghil, M., Halem, M., and Atlas, R. 1979. Time-continuous assimilation of remote-sounding data and its effect on weather forecasting. *Mon. Weather Rev.*, **107**(2), 140–171.
- Hoyer, J. L. and She, J. 2007. Optimal interpolation of sea surface temperature for the North Sea and Baltic Sea. *J. Marine Syst.*, **65**(1), 176–189.
- Ide, K., Courtier, P., Ghil, M., and Lorenc, A. C. 1997. Unified notation for data assimilation: operational, sequential and variational. *J. Meteorol. Soc. Jpn. Ser. II*, **75**(1B), 181–189.
- Ivanov, S. V., Kosukhin, S. S., Kaluzhnaya, A. V., and Boukhanovsky, A. V. 2012. Simulation-based collaborative decision support for surge floods prevention in St. Petersburg. *J. Comput. Sci.*, **3**(6), 450–455.
- Kalman, R. E. and Bucy, R. S. 1961. New results in linear filtering and prediction theory. *J. Basic Eng.*, **83**(3), 95–108.
- Kikas, V. and Lips, U. 2016. Upwelling characteristics in the Gulf of Finland (Baltic Sea) as revealed by Ferrybox measurements in 2007–2013. *Ocean Sci.*, **12**(3), 843–859.
- Laanemets, J., Väli, G., Zhurbas, V., Elken, J., Lips, I., and Lips, U. 2011. Simulation of mesoscale structures and nutrient transport during summer upwelling events in the Gulf of Finland in 2006. *Boreal Environ. Res.*, **16**, 15–26.
- Lagemaa, P. 2012. *Operational Forecasting in Estonian Marine Waters*. TUT Press.
- Lips, U., Lips, I., Kikas, V., and Kuvaldina, N. 2008. Ferrybox measurements: a tool to study meso-scale processes in the Gulf of Finland (Baltic Sea). In *2008 IEEE/OES US/EU-Baltic International Symposium, 27–29 May 2008, Tallinn, Estonia*, pp. 334–339.
- Lips, U., Kikas, V., Liblik, T., and Lips, I. 2016. Multi-sensor in situ observations to resolve the sub-mesoscale features in the stratified Gulf of Finland, Baltic Sea. *Ocean Sci.*, **12**(3), 715–732.
- Liu, Y., Zhu, J., She, J., Zhuang, S., Fu, W., and Gao, J. 2009. Assimilating temperature and salinity profile observations using an anisotropic recursive filter in a coastal ocean model. *Ocean Model.*, **30**(2), 75–87.
- Liu, Y., Meier, H. E., and Axell, L. 2013. Reanalyzing temperature and salinity on decadal time scales using the Ensemble Optimal Interpolation data assimilation method and a 3D ocean circulation model of the Baltic Sea. *J. Geophys. Res. Oceans*, **118**(10), 5536–5554.
- Liu, Y., Meier, H. M., and Eilola, K. 2014. Improving the multiannual, high-resolution modelling of biogeochemical cycles in the Baltic Sea by using data assimilation. *Tellus A*, **66**, 24908.
- Lorenc, A. C. 1986. Analysis methods for numerical weather prediction. *Q. J. Roy. Meteor. Soc.*, **112**(474), 1177–1194.
- Losa, S. N., Danilov, S., Schröter, J., Nerger, L., Maßmann, S., and Janssen, F. 2012. Assimilating NOAA SST data into the BSH operational circulation model for the North and Baltic Seas: inference about the data. *J. Marine Syst.*, **105**, 152–162.
- Losa, S. N., Danilov, S., Schröter, J., Janjić, T., Nerger, L., and Janssen, F. 2014. Assimilating NOAA SST data into BSH operational circulation model for the North and Baltic Seas: Part 2. Sensitivity of the forecast's skill to the prior model error statistics. *J. Marine Syst.*, **129**, 259–270.
- Martin, M., Dash, P., Ignatov, A., Banzon, V., Beggs, H., Brasnett, B., et al. 2012. Group for High Resolution Sea Surface temperature (GHRSSST) analysis fields inter-comparisons. Part 1: A GHRSSST multi-product ensemble (GMPE). *Deep Sea Res. Part II Top. Stud. Oceanogr.*, **77**, 21–30.
- McPherson, R. D., Bergman, K. H., Kistler, R. E., Rasch, G. E., and Gordon, D. S. 1979. The NMC operational global data assimilation system. *Mon. Weather Rev.*, **107**(11), 1445–1461.
- Nardelli, B. B., Tronconi, C., Pisano, A., and Santoleri, R. 2013. High and Ultra-High resolution processing of satellite Sea Surface Temperature data over Southern European Seas in the framework of MyOcean project. *Remote Sens. Environ.*, **129**, 1–16.
- Nowicki, A., Dzierzbicka-Głowacka, L., Janecki, M., and Kałas, M. 2015. Assimilation of the satellite SST data in the 3D CEMBS model. *Oceanologia*, **57**(1), 17–24.
- She, J., Hoyer, J. L., and Larsen, J. 2007. Assessment of sea surface temperature observational networks in the Baltic Sea and North Sea. *J. Marine Syst.*, **65**(1), 314–335.
- Siegel, H., Gerth, M., and Tschersich, G. 2006. Sea surface temperature development of the Baltic Sea in the period 1990–2004. *Oceanologia*, **48**(S), 119–131.
- Sokolov, A., Andrejev, O., Wulff, F., and Rodriguez Medina, M. 1997. *The Data Assimilation System for Data Analysis in the Baltic Sea*. Systems Ecology Contributions 3. Stockholm University.
- Soosaar, E., Maljutenko, I., Raudsepp, U., and Elken, J. 2014. An investigation of anticyclonic circulation in the southern Gulf of Riga during the spring period. *Cont. Shelf Res.*, **78**, 75–84.
- Sørensen, J. V. T. and Madsen, H. 2004. Efficient Kalman filter techniques for the assimilation of tide gauge data in three-dimensional modeling of the North Sea and Baltic Sea system. *J. Geophys. Res. Oceans*, **109**, CO3017.
- Tang, Y., Kleeman, R., and Moore, A. M. 2004. SST assimilation experiments in a tropical Pacific Ocean model. *J. Phys. Oceanogr.*, **34**(3), 623–642.
- Taylor, K. E. 2001. Summarizing multiple aspects of model performance in a single diagram. *J. Geophys. Res. Atmospheres*, **106**(D7), 7183–7192.
- Uiboupin, R. and Laanemets, J. 2009. Upwelling characteristics derived from satellite sea surface temperature

- data in the Gulf of Finland, Baltic Sea. *Boreal Environ. Res.*, **14**(2), 297–304.
- Uiboupin, R. and Laanemets, J. 2015. Upwelling parameters from bias-corrected composite satellite SST maps in the Gulf of Finland (Baltic Sea). *IEEE Geosci. Remote Sens. Lett.*, **12**(3), 592–596.
- Väli, G., Zhurbas, V., Lips, U., and Laanemets, J. 2017. Submesoscale structures related to upwelling events in the Gulf of Finland, Baltic Sea (numerical experiments). *J. Marine Syst.*, **171**, 31–42.
- Zhuang, S. Y., Fu, W. W., and She, J. 2011. A pre-operational three Dimensional variational data assimilation system in the North/Baltic Sea. *Ocean Sci.*, **7**(6), 771–781.

Mereandmete assimileerimise testimine Läänemere kirdeosas, kasutades Copernicuse mereseire programmi satelliitproduktide veepinna temperatuuri andmeid

Mihhail Zujev ja Jüri Elken

Katsetati Copernicuse mereseire programmi satelliitproduktide veepinna temperatuuri (SST) andmete assimileerimist piirkondlikku mereprognoside mudelisse HBM, mis oli seadistatud Läänemere kirdeosa jaoks, kaasa arvatud Soome ja Liivi laht. Igapäevastele prognoosidele ajavahemikus aprillist detsembrini 2015 rakendati kaht assimileerimise algoritmi: järjestikuseid parandusi ja optimaalinterpolatsiooni. Valideerimine oli tehtud Tallinna-Helsingi liinil sõitvate laevade pardalt kogutud FerryBoxi andmetega. Suuremad SST prognoosivead (kasutades assimileerimiseta referentsmudelit) esinesid väiksemate sügavustega looderanniku lähedal. Tuulevaiksete soojenemisperiodide jooksul, kevadel ja varasuvel, tekitas mudel soojema veemassi, kui näitasid satelliidi ning FerryBoxi andmed. Vaatlustega võrreldes külmemad piirkonnad olid modelleeritud hilissuvest talveni. Kuigi assimileerimise tulemusena õnnestus vigu vähendada, on otstarbekas parendada referentsmudeli osavust prognoosida veevahetust rannaala ja avamere vahel.